



Contents lists available at ScienceDirect

Surface Science

journal homepage: www.elsevier.com/locate/susc

The small unit cell reconstructions of SrTiO₃(1 1 1)

Laurence D. Marks^{a,*}, Ann N. Chiaramonti^a, Fabien Tran^b, Peter Blaha^b

^a Institute for Catalysis in Energy Processes and Department of Materials Science and Engineering, Northwestern University, 2220 N Campus Drive, Evanston, IL 60208, USA

^b Institute of Materials Chemistry, Vienna University of Technology, Getreidemarkt 9/165-TC, A-1060 Vienna, Austria

ARTICLE INFO

Article history:

Received 2 December 2008

Accepted for publication 10 April 2009

Available online xxx

Keywords:

DFT

Polar oxide surfaces

Surface structure

ABSTRACT

We analyze the basic structural units of simple reconstructions of the (1 1 1) surface of SrTiO₃ using density functional calculations. The prime focus is to answer three questions: what is the most appropriate functional to use; how accurate are the energies; what are the dominant low-energy structures and where do they lie on the surface phase diagram. Using test calculations of representative small molecules we compare conventional PBE–GGA with higher-order methods such as the TPSS meta-GGA and on-site hybrid methods PBE0 and TPSSH, the later being the most accurate. There are large effects due to reduction of the metal d oxygen sp hybridization when using the hybrid methods which are equivalent to a dynamical GGA + *U*, which leads to rather substantial improvements in the atomization energies of simple calibration molecules, even though the d-electron density for titanium compounds is rather small. By comparing the errors of the different methods we are able to generate an estimate of the theoretical error, which is about 0.25 eV per 1 × 1 unit cell, with changes of 0.5–1.0 eV per 1 × 1 cell with the more accurate method relative to conventional GGA. An analysis of the plausible structures reveals a new low-energy TiO₂-rich configuration with octahedral co-ordination. This structure can act as a template for layers of either TiO or Ti₂O₃, consistent with experimental results. The results also suggest that both the fracture surface and the stoichiometric SrTiO₃(1 1 1) surface should spontaneously disproportionate into SrO and TiO₂ rich domains.

© 2009 Elsevier B.V. All rights reserved.

1. Introduction

Oxides are ubiquitous as they are present on earth and in every soil and sediment as well as in aerosols, aquatic biota, and waste streams. They come from a variety of sources, both natural and anthropogenic. For most bulk oxides the crystal structures are well established, and for many systems the thermodynamics are well documented from experiments and theoretical calculations. At the surface much less is understood. While one can easily perform theoretical calculations on simple bulk-like (e.g. 1 × 1) terminations, the actual thermodynamically stable surface and/or experimentally observed structures are often larger and more complicated. Until these surface structures have been unambiguously experimentally determined, the problem can be confused. Even for such a simple system as the (1 0 0) surface of the archetypal perovskite strontium titanate, there are at least six different experimentally determined surface reconstructions in addition to the simple 1 × 1 bulk terminations. Not all of these structures have yet been solved at the atomic level, and to date there is not convincing agreement between experimental observations and theoretical analyses as to which surface structures should be stable under what conditions.

More complicated yet is the problem of the so-called polar surfaces. These are surfaces where a simple Gibbs truncation to form a 1 × 1 structure leads, in a fully ionic model, to a surface with a nett charge and/or an unbalanced macroscopic dipole which would lead to an infinite surface energy. For an isolated surface in vacuum or a gas, except for special cases where charge has deliberately been created (for instance with a Van Der Graaff generator), the nett charge of a true surface is always zero and the energy will never be infinite. There has been extensive discussion of the mechanisms of “charge compensation” for oxide surfaces in the literature (see for instance [1,2] and references therein), but typically they assume a fully ionic model, which is not correct in the case of many transition metal oxides. A nice, very recent demonstration of this is the analysis by Raebiger et al. of charge self-regulation in transition metal ions in semiconductors [3]. An alternative concept is to consider what we will refer to as “valence compensation”. Attributing a nominal charge equal to the valence of each atom type, if this is nett zero, is likely to give an insulator with a relatively large band-gap; if not there will probably be either n-type or p-type states. Since the band-gap in many oxides is large in most cases the extra energy associated with creating a hole in the valence band would make the surface a stronger oxidant than molecular oxygen; an electron in the conduction band well capable of reducing water. This is physically unlikely so in many cases the polar surfaces will rearrange to form more stable and redox neutral configurations.

* Corresponding author.

E-mail address: l-marks@northwestern.edu (L.D. Marks).

A very specific case is the SrTiO₃(1 1 1) surface. A wide range of reconstructions have been observed depending upon the annealing time (on the scale of hours), the temperature, the oxygen partial pressure, and whether the specimens were ion beam sputtered before analysis including (1 × 1) [4–6], (9/5 × 9/5) [7–9], (√7 × √7 R19.1°) [10], (3 × 3) [7–9], (√13 × √13 R13.9°) [10], (4 × 4) [7–9], (5 × 5) [9], (6 × 6) [7–9] as well as a TiO overgrowth under highly reducing conditions [9]. While the approximate chemistry and morphology of the surfaces is relatively well characterized, nobody has yet proposed and verified an atomic-level structure solution which includes locating the three-dimensional positions of all the atoms in the reconstructed surface selvedge and verifying the result with structure refinement and/or simulation against scattering data. There is only one theoretical study in the literature using a semi empirical Hartree–Fock method [11,12], and this considered a few relatively simple 1 × 1 and 2 × 1 structures, not the much larger reconstructed cells observed experimentally or other possibilities that we will discuss later.

It has now become almost conventional when proposing a model for a surface reconstruction to perform a density functional theory (DFT) calculation. What one wants to know is whether the proposed positions are plausible, i.e. the difference between them and refined DFT positions is not too large, as well as whether energetically the structure is plausible. For this one needs to have answered three fundamental questions:

- (1) What is the most appropriate DFT functional to use; there are many in the literature.
- (2) What are the errors in the energies? These numbers are rarely analyzed or published and from an experimental viewpoint a measurement without errors is marginal. Obviously only with knowledge of the errors in the energies can one determine if a structure is plausible.
- (3) What are the basic simple structures against which one wants to compare a reconstruction? Since often reconstructions are variants/superstructures based upon simple 1 × 1 units, this information is also needed *a-priori* to aid in solving reconstructions, particularly ones with large unit cells such as observed for the (1 1 1) surface of SrTiO₃.

The focus of this paper is to provide some answers to the three questions above for the (1 1 1) surface of SrTiO₃; the more complicated $n \times n$ reconstructions is a topic of further publications. The structure of the paper is as follows. After a brief, technical description of the parameters used, we turn to an analysis of what functional to use. Our approach is to analyze the atomization energies of some representative small molecules, as a reasonable model for changes in bonding at a surface (which dominate the relative surface energies). We point out that even though titanium has a rather small d-electron population it is important to consider higher-order methods which compensate for inaccuracies in the d-electron exchange–correlation potential. An efficient method of doing this is an on-site hybrid-DFT (PBE0) method, where one adds a fraction of exact exchange (inside sphere and only for selected electrons) and which is similar to a GGA + U method but with a dynamically calculated Hubbard U term. The best results are obtained using a meta-GGA combined with a hybrid functional. By comparing the errors for different functionals for these known cases, we can estimate that the theoretical error for the surface energies in terms of the difference in the results for different functionals. We then turn to the basic structures, including a number of not-so-simple 1 × 1 reconstructions on the TiO_x-rich part of the surface phase diagram. We find a low-energy structure with octahedral co-ordination which obeys the rules of solid-state chemistry, similar to what has been found for SrTiO₃ (0 0 1) [13]. This structure acts as a ready template for additional growth of TiO or

Ti₂O₃ layers, consistent with experimental results. These results are combined into a partial phase diagram of the simple structures.

2. Methods and computational details

For the DFT calculations the all-electron Wien2k code [14] with an augmented plane wave (APW) basis set was employed. For reference, technical parameters were: atomic sphere sizes (RMT's) of 2.36, 1.72 and 1.54 a.u. for Sr, Ti and O, respectively, a Fourier series cutoff of GMAX = 21.6 for the charge density and potential, and a wavefunction cutoff (defined as product of the smallest RMT times the largest K in the plane wave expansion) of RKMAX = 6.12. The Brillouin zone sampling was 5 × 5 × 1 for the 1 × 1 cell, scaled for the larger cells to retain approximately the same density of points in reciprocal space. A small (0.0018 Rydberg) temperature factor corresponding to the Fermi–Dirac occupation at room temperature was used; this had little effect since most of the relevant structures were insulators. The separation between the two surfaces was at least 1 nm, with total slab sizes of 2–2.5 nm. Tests indicated that the intrinsic numerical errors such as convergence as a function of reciprocal-space sampling were <0.01 eV per 1 × 1 unit cell, which is much smaller than the variations with different functionals as detailed below. In all cases the surface energies were determined by subtracting the appropriate energies for bulk SrTiO₃, SrO or TiO₂, calculated in larger supercells (for instance a hexagonal cell with $a = [1 1 0]$ and $c = [1 1 1]$ for SrTiO₃) with matching technical parameters to minimize numerical errors. Although initial calculations were performed using the conventional generalized gradient approximation (GGA) as defined by the PBE functional [15], for reasons that we will discuss in more detail below for the final calculations we used an on-site Hartree–Fock hybrid method [16,17], namely the PBE0 functional [18,19] for the exchange–correlation potential, while the exchange–correlation energy is taken from the meta-GGA TPSS functional [20], equivalent to an on-site TPSSh method [21]. In this context on-site means that the exact-exchange (Hartree–Fock) part is calculated only for selected electrons (Ti-3d) inside the corresponding Ti sphere [17], thus keeping the numerical effort quite small. For reference, both PBE and the TPSS calculations were performed with the PBE minimized lattice parameters, while the PBE0 and TPSSh results were obtained with the refined lattice parameters for PBE0.

3. Choice of DFT method

While DFT calculations to accompany experimental surface structure analyses have become common, one has to be careful when performing such correlations. Particularly in the case of oxides, the method must do a reasonable job of taking account of not simply the bulk bonding, but how the covalent and ionic bonding changes at a surface as well as the long-range surface energy contributions. The earliest functional to be used was LDA (e.g. [22]). While this sometimes gives relatively good surface energies and other results due to a fortuitous cancellation (e.g. [20–22]), the failings of the LDA are now well established. The most common functional currently used is the PBE GGA [15], which while it often gives very good results, still has some problems particularly for energies. For instance, it is now well established that it severely underestimates surface energies [23–25]. In addition, for many bulk transition element oxides there is too much hybridization between the metal 3d-electrons and the oxygen 2sp, and the classic method for correcting this is what has become known as the LDA + U method [26,27]. In general LDA + U increases the ionicity of the bonding, which can be badly underestimated otherwise. The method requires a number for the value of the Hubbard U that is difficult to determine independently and will depend upon the

local environment so is not a global parameter. While one would not normally consider SrTiO₃ or insulating compounds containing Ti as cases where one has to use this method (because the d-electron density is small), even here there is a noticeable hybridization between the oxygen 2sp levels and the Ti d-levels.

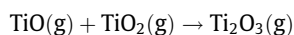
A recently developed alternative to the LDA + *U* method, which involves less in the way of arbitrary parameters, is to use an on-site hybrid [17] based upon an approach such as the PBE0 functional [18,19]. One adds a small component of exact-exchange for the relevant Kohn–Sham orbitals (d-electrons only here), which can be calculated rather simply within the muffin tin radii of an APW method. It has been shown [17] that this is similar to a LDA/GGA + *U* method, but with a *U* value that is dynamically calculated and will vary with environment. Strictly speaking the appropriate amount of exact-exchange is system dependent but in many cases a fixed value works, for instance 0.25 for the PBE0 functional (see also the discussion). This is important because it removes the issue of what value of *U* is relevant for a surface atom as against a bulk atom since they are different; one uses a fixed value for the amount of exact exchange and the calculation automatically adjusts the effective *U* value depending upon the environment. In addition, a method for calculating the forces has recently been developed [28] so the on-site method can be applied for a full structural minimization with at most a 10% overhead relative to a conventional GGA calculation; indeed in some cases because the Hamiltonian is better posed the method can be faster than a conventional GGA, because the SCF iterations may converge faster [29]. As such it is much faster than methods which use a full or screened calculation of the exact exchange term.

While the on-site hybrid approach appears to be better for energies (see below), we can go a bit further. As mentioned above, the PBE functional gives poor surface energies. A much better method for this is the TPSS meta-GGA functional [20] which includes beside the gradient of the density also the kinetic-energy density in the functional form which is known to match quite well the long-range jellium surface energies which are believed to be an issue with PBE [23–25]. TPSS also gives much better atomization energies for molecules. It corrects, for instance, the overestimation of the atomization energy for O₂ which is ~6.5 eV with PBE whereas TPSS gives ~5.3 eV, a value that is closer to the experimental result of 5.12 eV (e.g. [30]). While it is hard to implement this functional in a fully self-consistent fashion it is common practice to use the electron density corresponding to e.g. a PBE potential and includes only the exchange–correlation energy contribution and this is known to give quite similar results (as suggested first in the original publication [20]). A combination of full TPSS and PBE0 is called the TPSSh functional; the on-site version will be referred to as an on-site TPSSh method [21]. (The original papers used the TPSSh functional with a small amount of exact exchange, 0.1; for the on-site implementation the same value as for PBE0 of 0.25 works better at least for the systems studied herein.)

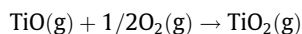
For completeness, we also tested a recent one-parameter optimization of TPSS [31]. While this gave slightly better atomization

energies, the difference was small and slightly worse for the disproportionate reaction so it will not be used here.

To verify that the on-site method is an improvement, the atomization energies of a number of small Ti + O molecules for which experimental data are available (see [32,33] and references therein) were calculated, with the experimental values corrected for the zero-point energies. To understand the limits of applicability, the data for TiN was also included, (see [34] and references therein) where the calculated values particularly with TPSSh are not as accurate as they are for the other compounds; the method is not perfect. The indirect DFT band-gap of bulk SrTiO₃, which is of course not the same as the true band-gap of 3.77 eV [35], but representative of it, was also examined. Since for TPSS and TPSSh functionals we do not have a self-consistent electronic structure, the gap was estimated from the total energies by modifying the Fermi–Dirac occupancy so that N- δ electrons were below the valence-band edge and δ above the conduction-band edge, and iterating to self consistency. (For completeness, this gave identical values for the band-gap for PBE as one would obtain from the difference between the lowest unoccupied highest occupied eigenvalues.) As it is sometimes argued that the isolated atom reference energies lead to errors in atomization energies, we also considered the decomposition reaction for which the experimental value per molecule is 5.48 (see [32,33] and references therein).



the oxidation reaction (experimental value –3.60 eV)



and lastly the formation reaction for which the experimental value is 1.425 eV [36]:

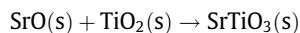


Table 1 summarizes the results, with the common hybrid method B3PW91 [37] (on-site form) as well as the older LDA method included for reference. We can rank the accuracy of the methods as LDA << PBE << TPSS ~ PBE0 << TPSSh, except for TiN where PBE0 is best, although even with TPSSh the absolute errors in the energies are still significant. We note that the overall trend of the accuracy is consistent with what has been found in recent comparable tests using the rather slower approach of applying the exact-exchange term to all electrons, e.g. [34,38–41]. We also show in the table the effective Bader's "atoms in molecules (AIM)" theory [42] charge on the oxygen for SrTiO₃ as well as results for an effective Hubbard-*U* parameter *U*_{eff} obtained from an L2 fit of the orbital potential versus a conventional *U* method with *J* = 0, which in this case works well with an RMS error of ~0.15 although we should caution that in some other cases (e.g. an isolated Ti atom, RMS error ~0.7) it is not a good description. As one would expect the *U*_{eff} value increases as the electron density around the Ti atom decreases, i.e. the shielding of the d-electrons decreases.

A brief additional discussion of these numbers is useful; most of the conclusions we make are relatively well known in the litera-

Table 1

Errors in the atomization energies per atom of some small Ti + O as well as TiN test molecules, the effective values of the L2 fit Hubbard *U* constant, the error in the energy for the decomposition reaction, gas-phase oxidation of TiO to TiO₂, formation of SrTiO₃ from SrO and TiO₂ the indirect band gap (experimentally 3.77 eV [35]) at the DFT equilibrium lattice parameter, as well as the Bader-charge on the oxygen in SrTiO₃, all energies in eV. For Ti₂O₃ the smaller value of *U* is for the 2-fold coordinated Ti, the larger for the 3-fold coordinated.

	TiO	TiO ₂	Ti ₂ O ₃	TiN	Decomposition	Oxidation	Formation	Gap	Ionicity
LDA	1.08	1.32	1.11	0.86	0.12	-0.22	0.06	1.83	1.25
PBE	0.60	0.58	0.31	0.34	0.28	-0.01	0.21	1.83	1.27
B3PW91	0.45	0.50	0.28	0.15	0.20	0.00	0.46	2.30	1.31
TPSS	0.46	0.40	0.17	0.09	0.26	-0.03	0.05	2.24	1.27
PBE0	0.32	0.43	0.20	0.12	0.19	-0.05	0.22	2.15	1.32
TPSSh	0.13	0.19	0.03	-0.21	0.14	-0.04	0.08	2.40	1.32
<i>U</i>	4.93	5.87	4.85, 5.61	5.53					

ture. Due to the neglect of self-interaction correction the LDA method often has, as for the oxides here, too much covalent bonding, and not enough ionicity which leads to the overbonding of the TiO_x molecules. It is known that sometimes the inherent errors in the exchange and correlation terms in LDA cancel, so one could make arguments for its use iff all compounds are very similarly bonded. However, as mentioned earlier, we need a good representation of *both* the covalent and ionic components for a surface particularly if the bonding changes (see also later). The PBE functional does a better job, making the system more ionic and reducing the excess covalency but it is still too strongly covalently bonded. The meta-GGA improves upon the covalency. As implemented here it cannot have any effect on the ionicity, but there is data in the literature from fully self-consistent meta-GGA calculations which indicate that in general it has only a small effect upon the ionicity (e.g. [43,44]). Adding in some exact-exchange improves the description of the exchange component of the energy and potential, increasing the ionicity, and in many cases improving the results (albeit not for metals where the loss of balance between the exchange and correlation contributions in a hybrid method can make the results worse). Combining the better description of ionicity and covalency in a hybrid meta-GGA gives the best results in many cases.

The on-site method has not previously been tested extensively for the energies, and it is encouraging that this approximation gives rather good energies. Perhaps surprising is that it has such a large effect since the total d-electron density is only about one electron per titanium atom. The correction to the exchange energy and potential shifts up the energy of the d-electrons, reducing the degree of hybridization of the oxygen 2sp levels with the titanium 3d and as a consequence making the bonding more ionic. One can estimate the ionic charges using Bader's "atoms in molecules (AIM)" theory [42], which for bulk TiO_2 gives a nominal Ti charge of +2.28 with PBE versus +2.43 with PBE0. For completeness we note that the fact that conventional PBE calculations underestimate the ionicity of systems containing Ti is supported by other experimental evidence such as charge density data [45].

The calculations of the energies for the small molecules is not perfect, neither will be the energies for surfaces. We need to have

an estimate of the error to be able to determine anything. From Table 1 a reasonable estimate is to take $\sigma = |E_{\text{TPSSH}} - E_{\text{PBE}}|/3$.

4. Calculated $T = 0$ K energetics

Fig. 1 summarizes the compositions of the different structures in terms of a surface analogue of a conventional three-component phase plot. While the energies for the (less accurate) PBE method are qualitatively similar to what is found with the TPSSH method, because the later appear to be much more accurate only those are reported. In detail, the specific structures were:

- (1) Models 1 and 2, a simple bulk-terminated (1 1 1) SrTiO_3 1×1 surface, both Ti (Model 1, Fig. 2a) and SrO_3 terminations (Model 2, Fig. 2b). In these and all subsequent figures the titanium co-ordination is shown using a polyhedral representation with the Ti atoms red, oxygen light blue and strontium dark blue. Neither of these are stoichiometric, the Ti termination being Ti rich and oxygen deficient (n-type) whereas the SrO_3 termination is oxygen and strontium rich (p-type). Contrary to the earlier semi-empirical calculations we find that both of these are metallic in nature as one would expect.
- (2) Model 3, a valence compensated SrO termination (SrO rich) which corresponds to a $c2 \times 1$ reconstruction with oxygen vacancies in the surface as shown in Fig. 2c, similar to that analyzed by Pojani et al. [11,12]. This structure contains octahedral TiO_5 units (where \square denotes a missing oxygen) so can be expected to be relatively stable [13].
- (3) Model 4, a valence compensated 1×1 TiO termination (TiO_2 rich) with a tetrahedrally coordinated surface Ti atom with an oxygen atom above it, shown in Fig. 2d, similar to that analyzed by Pojani et al. [11,12].
- (4) Models 5 and 6, two possible valence compensated SrTiO_3 terminations with half the Ti atoms missing in the outermost Ti layer, with 5 shown in Fig. 2e (a 2×1 cell) and 6, in Fig. 2f (a 2×2 cell).

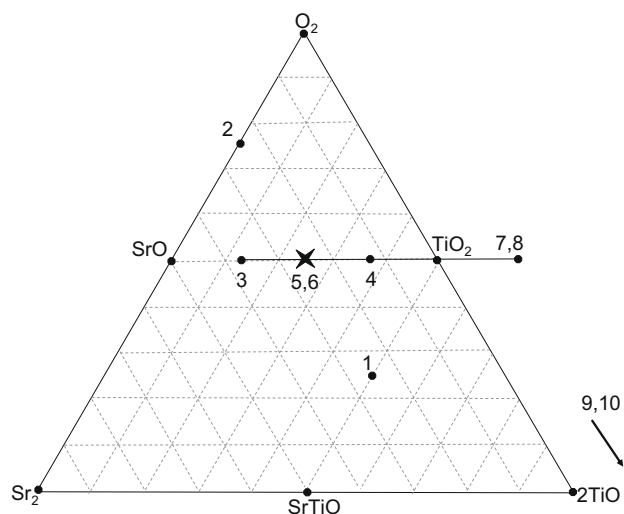


Fig. 1. Surface analogue of a three-component phase plot. The compositions indicated correspond to monolayer excesses of the corresponding species with a stoichiometric SrTiO_3 marked by the cross. The various models are marked by numbers. The horizontal line is the locus of valence compensated structures; above are oxidized, below reduced.

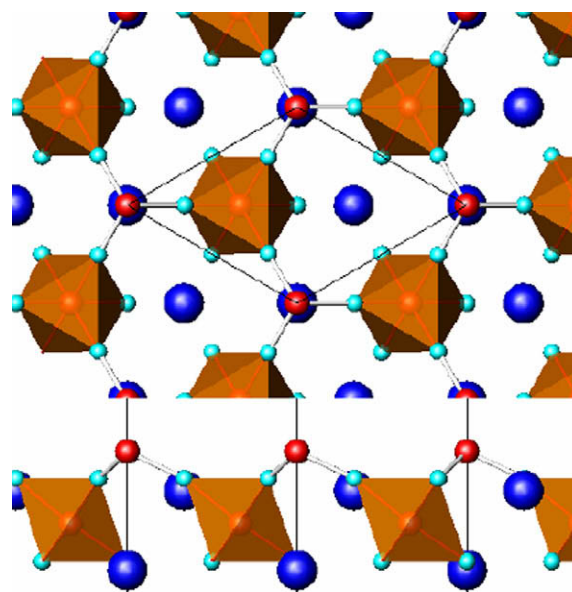


Fig. 2a. Model 1, non valence-neutral Ti terminated surface from above (top) and from the side (below). In this and all subsequent figures the titanium co-ordination is shown using a polyhedral representation (brown polyhedra) with the Ti atoms red, oxygen light blue and strontium dark blue. (For interpretation of the references to colour in this figure legend, the reader is referred to the web version of this article.)

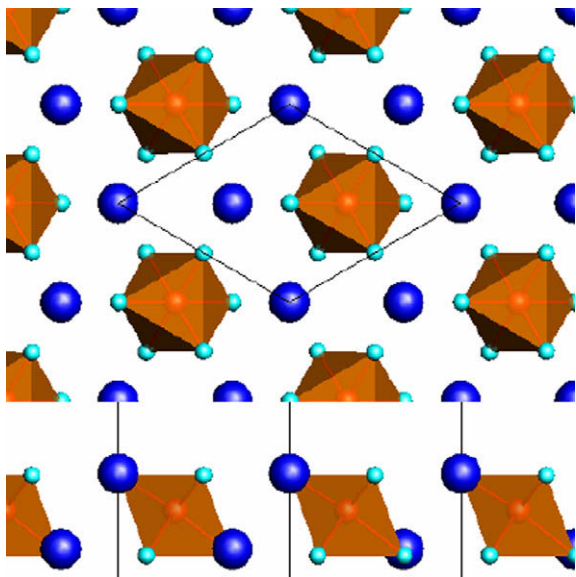


Fig. 2b. Model 2, non valence-neutral SrO_3 terminated surface from above (top) and from the side (below).

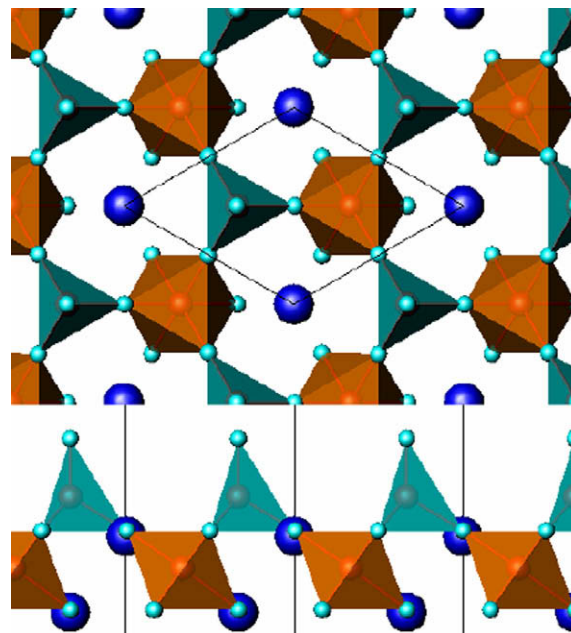


Fig. 2d. Model 4, valence compensated 1×1 TiO terminated surface with tetrahedral Ti at the surface (dark green) from above (top) and from the side (below). (For interpretation of the references to colour in this figure legend, the reader is referred to the web version of this article.)

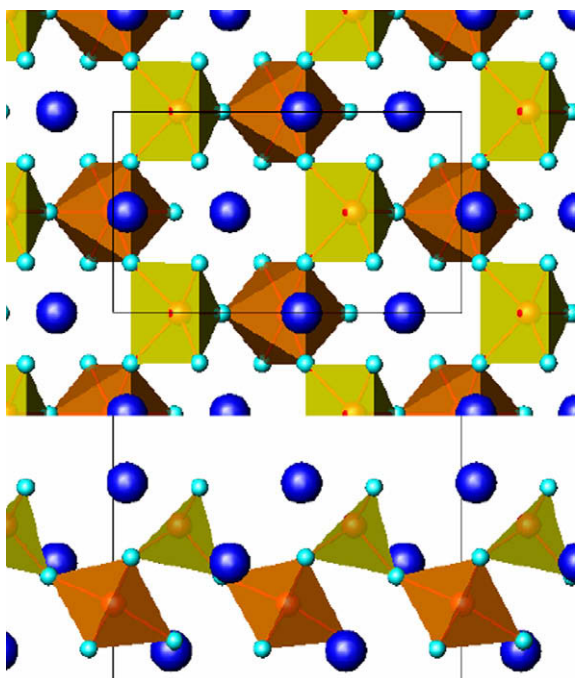


Fig. 2c. Model 3, a $c2 \times 1$ valence compensated surface with 20 vacancies per surface cell, and square pyramidal Ti at the surface (light green) from above (top) and from the side (below). (For interpretation of the references to colour in this figure legend, the reader is referred to the web version of this article.)

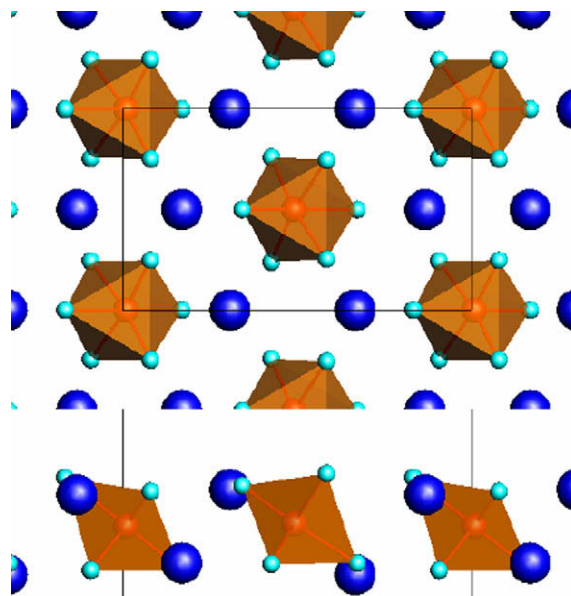


Fig. 2e. Model 5, valence compensated $c2 \times 1$ Ti terminated surface with 2 Ti vacancies per unit cell from above (top) and from the side (below).

- (5) Model 7, a TiO_2 rich valence compensated 1×1 reconstruction with a Sr vacancy in the 2nd layer, Fig. 2g.
- (6) Model 8, (Fig. 2h) a TiO_2 rich valence compensated 1×1 reconstruction where in addition to a Ti atom in the normal position at the surface, another is placed above one of the Ti atoms in the layer below and the structure is terminated with a layer of oxygen atoms. This structure has octahedrally coordinated titanium at the surface, with half face-sharing with respect to the layer below. As such this structure obeys the rule for preferred octahedral co-ordination previously proposed for SrTiO_3 (0 0 1) surfaces [13].

- (7) Models 9 and 10, two more TiO_x rich structures based upon adding layers to Model 8. In Model 9 (Fig. 2i, left) the additional layer has a stoichiometry of Ti_2O_3 which for Model 10 (Fig. 2j right) it is $3(\text{TiO})$, and both are 1×1 cells. For the Ti_2O_3 structure two of the three possible 3-fold sites above the terminal oxygen layer of Model 8 are occupied, for the TiO structure all three.

Refined positions for these different models are available as conventional crystallographic cif files [46]. An analysis of aspects of the lower-energy structures will be given later in the discussion.

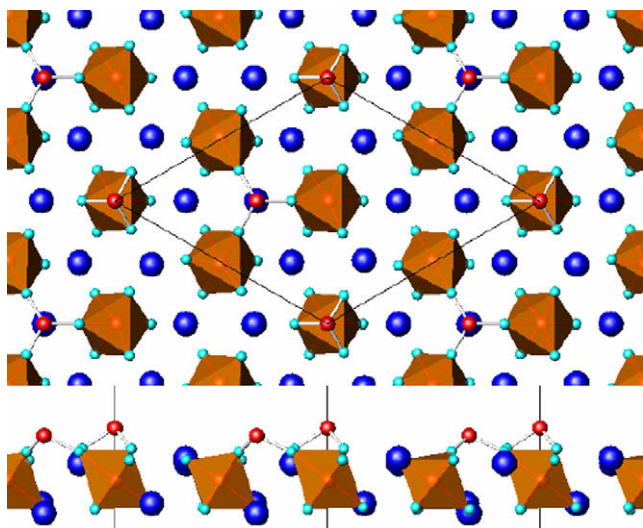


Fig. 2f. Model 6, valence compensated 2×2 Ti terminated surface with 50% Ti vacancies from above (top) and from the side (below).

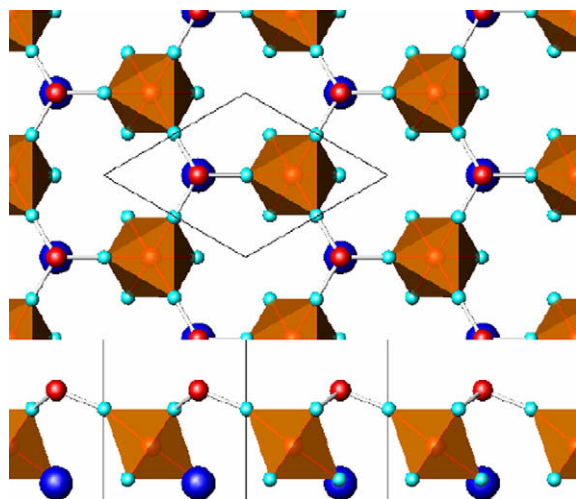


Fig. 2g. Model 7, valence neutral 1×1 cell with a Sr vacancy in the second layer from above (top) and from the side (below).

Two additional combinations of structures are important. The first is what we will call the bulk termination, generated by performing a planar cut of the bulk. This will be the average of the simple 1×1 terminations of Models 1 and 2. The second is the “Fracture Surface” which we define as the lowest energy combination of two structures which with minimal relaxations can be combined to form a perfect bulk. For this system this is the average of the oxygen vacancy Model 3 and the oxygen adatom Model 4. For completeness, note that the energy of the Fracture Surface will be close to the true fracture energy of the sample on a $(1\ 1\ 1)$ plane, and as such is amenable to experimental measurement; the fracture energy should be slightly higher than the number here due to residual plastic deformation contributions.

Shown in Table 2 are the surface energies per 1×1 unit cell for all the structures analyzed and the functionals PBE, PBE0, TPSS and TPSSh, referenced to bulk SrTiO_3 plus the relevant fractions of bulk TiO_2 and O_2 . There are several ways to interpret the data. A conventional method would be to use an *ab-initio* thermodynamics method (e.g. [47,48]) and plot the energies versus the chemical potential

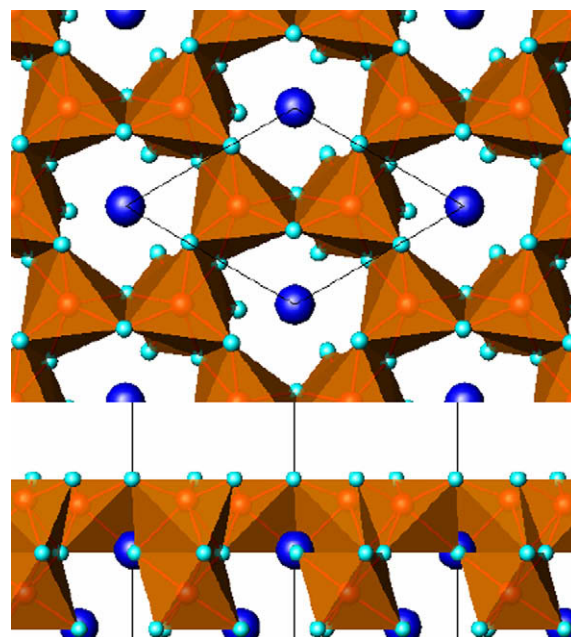


Fig. 2h. Model 8, a valence compensated TiO_2 rich 1×1 cell with octahedra at the surface from above (top) and from the side (below).

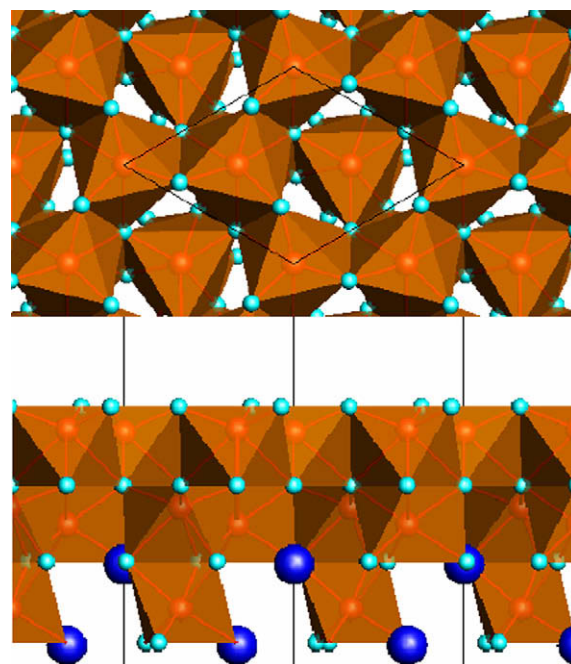


Fig. 2i. Model 9, Ti_2O_3 surface by stacking octahedra onto Model 8 from above (top) and from the side (below).

of the components or just that of TiO_2 taking the chemical potential of SrTiO_2 as a reference (via the disproportionation energy) to determine the chemical potential of SrO and plot a stability diagram, e.g. [49,50]. This is not wrong, but has some assumptions which are hard to justify in terms of most experiments. In general the surface of a SrTiO_3 sample is not in equilibrium with any source of TiO_2 or SrO to fix the chemical potential. While in principle it is in equilibrium with bulk vacancy clusters of SrO and TiO_2 , at the temperatures of experimental interest the kinetics are sluggish. In-

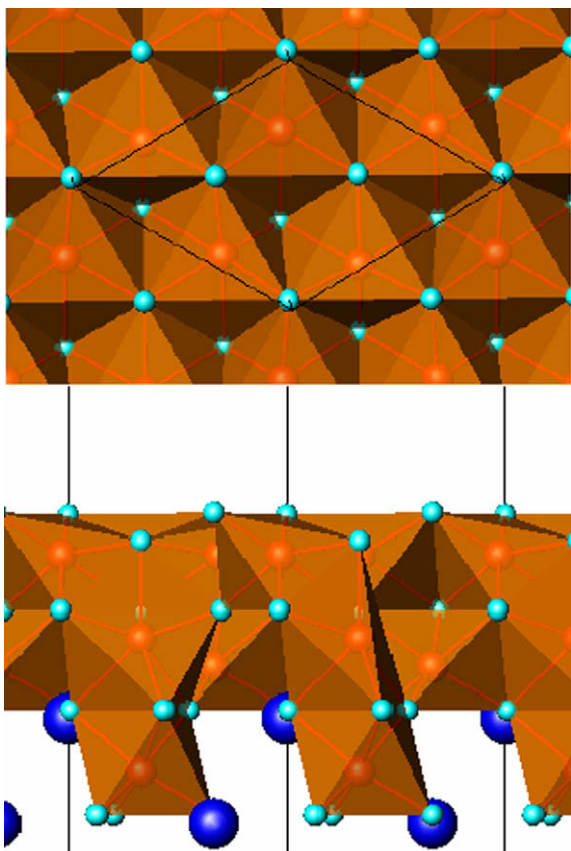


Fig. 2j. Model 10, TiO surface obtained by packing octahedra onto Model 8 from above (top) and from the side (below).

deed, the surface structures depend upon the history of treatment of the sample, particular annealing time and oxygen pressure [7,8]. We note that even with respect to oxygen we should not assume global equilibrium, rather only local equilibrium similar to the TiO_2 (0 0 1) surface [51].

For a local equilibrium analysis, which will be more relevant for most experiments, we consider the energetics for a fixed surface excess of TiO_2 , SrO and O and then calculate which combination of structures are thermodynamically of lowest energy; implicitly we assume that the composition may be determined by kinetics. For simplicity (it does not matter, see below) we set the chemical potential of both SrTiO_3 and TiO_2 as zero and plot the energies ver-

sus composition for all the non-reduced or oxidized structures as shown in Fig. 3. We then do a conventional convex-hull construction (as for bulk alloy thermodynamics), connecting all points on an energy-composition diagram and take the lowest energy combination; for structures containing either excess or less oxygen one can similarly perform a multidimensional convex-hull construction. The combination of phases can then be determined by a conventional lever-law at any composition. It should be noted that an advantage of the convex-hull construction is that if, for instance, we change the chemical potential of TiO_2 this simply linearly shifts the energies and has no effect upon the predicted phases.

The results are shown in Fig. 3 for the valence compensated compositions relative to the SrO-rich Model 3 for both PBE and TPSSh. With an estimate of the error as mentioned earlier, excluding the non-stoichiometric Models 1 and 2 (to avoid issues with the oxygen molecule bonding), we can estimate a value of $0.25 \text{ eV}/1 \times 1$ unit cell which has been used in the figure. While it is clear that if one compares relative energies the two different functionals give qualitatively comparable results, there are clearly rather large differences in the quantitative numbers (even when, as in this figure, an offset of 0.84 eV has been eliminated).

The analysis indicates that (of the structures considered) the stable phases are the SrO-rich Model 3 with TiO_5 units and the structure with complete octahedral TiO_6 units of Model 8 close to zero oxygen chemical potential; under highly oxidizing conditions the two bulk truncated 1×1 terminations and under highly reducing conditions the Ti_2O_3 or TiO overgrowths. The valence compensated structures follow the rules previously described for the SrTiO_3 (0 0 1) surface [13]. This is summarized in Fig. 4, excluding to two highly TiO_x rich structures. For completeness, we can only base an analysis on the phases considered, and others might be relevant. Note that the results indicate that the stoichiometric SrTiO_3 reconstructions as well as the fracture surface should disproportionate, with a 1.5σ (90%) confidence.

Some analysis of the effect of moving from the PBE functional to PBE0 and TPSSh is appropriate at this point. Several observations can be made:

- (1) The surface energies increase in the order $\text{PBE} < \text{PBE0} \sim \text{TPSS} < \text{TPSSh}$. The increase with PBE0 is in part because the system overall has become more ionic, and because the PBE method will be overestimating the possible covalent stabilization of the surface. The increase in the energy with the use of the meta-GGA TPSS is expected, and is one of the well-established problems with PBE. As a first approximation the ratio of the surface energies $E_{\text{TPSSh}}/E_{\text{PBE}}$ is ~ 1.3 with an accuracy of $\sim 0.1 \text{ eV}$ per 1×1 unit cell.

Table 2

Surface energies per 1×1 unit cell in eV as well as other information for the different models considered, for Models 1 and 2 at zero oxygen chemical potential for an O_2 atomization energy of 5.35 eV . The composition (Comp) is the number of surface excess units of TiO_2 less the number of surface excess SrO per 1×1 unit cell. Also shown in the table is the number of layers, atoms, the increase in the effective U value ($U_0 = 4.93 \text{ eV}$ in the bulk) at the surface in eV, the oxidation states relative to $1/2\text{O}_2$ and the two-dimensional symmetry.

Model	PBE	TPSS	PBE0	TPSSh	Composition	Layers	Atoms	dU	Oxid	Symmetry
1	7.11	7.26	7.98	8.37	0.5	13	31	0.43	-0.5	p3m1
2	3.05	3.71	3.22	3.92	-0.5	13	34	0.00	0.5	p3m1
3	2.37	2.63	2.64	3.00	-0.5	13	32	0.26	0	cm
4	2.57	2.88	2.84	3.41	0.5	15	38	0.43	0	p3m1
5	2.94	3.21	3.39	3.78	0	11	50	0.17	0	pm
6	3.35	3.68	3.89	4.37	0	11	100	0.43	0	p3m1
7	3.02	3.34	3.51	4.05	1.5	15	34	0.51	0	p3m1
8	1.66	1.76	2.00	2.31	1.5	15	44	0.17	0	p3
9	6.17	5.73	7.58	7.56	3.5	17	54	0.26	-0.5	p3
10	14.91	13.51	17.62	16.77	4.5	17	56	0.43	-1.5	p3
G	5.08	5.49	5.60	6.15	0				0	
F	2.47	2.76	2.74	3.20	0				0	

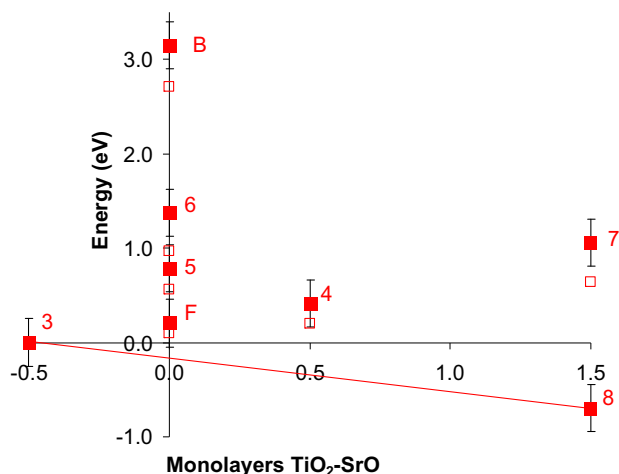


Fig. 3. Plot of the energies for the different valence compensated structures relative to the SrO-rich Model 3 as labeled, versus stoichiometry with an 0.25 eV error bar included, labeled with the relevant model; solid for TPSSh and empty for PBE. Also shown is the fracture surface energy (F), and the bulk termination (B), with the convex hull line shown in red. (For interpretation of the references to colour in this figure legend, the reader is referred to the web version of this article.)

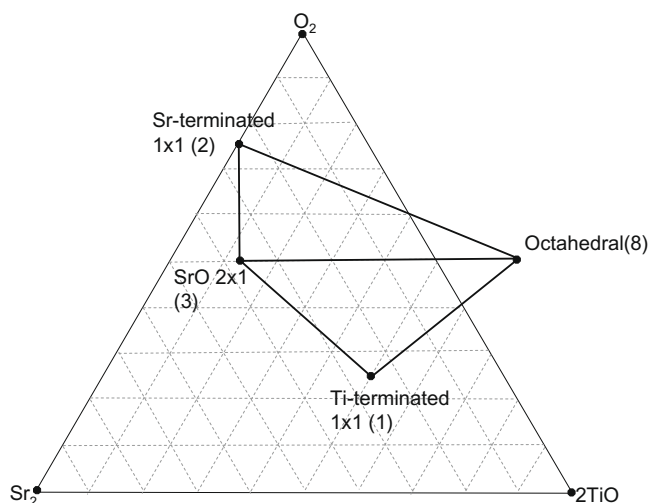


Fig. 4. Surface phase diagram, based upon the structures considered only.

- (2) The change in the enthalpies is not independent of which surface structure one has, and varies by as much as 0.5 eV between them. In general the increase is larger the higher the density of exposed titanium atoms at the surface, or the electron density in the d-levels as is the case for the n-type Ti terminated structure. This is exactly what one would expect for the increased ionicity.
- (3) While many features of Fig. 3 do not depend upon which functional is used, some do and in a predictable fashion. The largest effect is seen when one compares Model 7, a 1×1 with a missing Sr atom in the second layer, to the octahedral Model 8. This change is because Model 7 has an exposed Ti atom which is much more ionic when a better account is taken of the Ti-d, O-sp hybridization. It is fortuitous that (when normalized relative to Model 3) the octahedral model has the same relative energy in PBE and TPSSh. This is because both contain only octahedral Ti, so the changes in ionicity/covalency with the better functionals cancel out.

- (4) As one would expect, the effective U value ($U_0 = 4.93$ eV in the bulk) increases at the surface by 0.2–.5 eV with the exception of Model 2 where there is no change.

5. Discussions

We will discuss first the three questions which were posed in the introduction. There is a clear improvement when going from the standard GGA based upon the PBE method to the meta-GGA as well as the hybrid form, even the comparatively simple on-site implementation that we have used here. This is consistent with several recent analyses in the literature, e.g. [34,38–41]. While it turns out not to matter which functional one uses in terms of predicting the preferred structures, this is because the dominant structures in the SrO-rich and TiO₂-rich regimes have octahedral titanium so the errors cancel. Of course this will not be true in general. One issue is exactly how much of exact-exchange should be used. As analyzed in the original paper by Perdew, Ernzerhof and Burke [18] a value of 0.25 is close to optimum, but may not be best in all possible cases. For instance, for the NiO(1 1 1) surface which we will discuss elsewhere, a smaller value appears to be rather better for the Ni atoms, matching both the bulk properties as well as simple test molecules such as NiO, Ni(CO)₄ and Ni(CO)₃. What does appear to be the case is that this method has large advantages over conventional LDA + U as an auto-adjusting U method. While not easy, it should be possible to measure the relative surface energies experimentally particularly as a function of oxygen chemical potential to rather better than this level, so there may be some direct tests available.

It is worth repeating that the on-site PBE0 method has at most an additional 10% overhead relative to a conventional PBE-GGA. Indeed in some cases because the Hamiltonian is better posed the method can be faster than a conventional GGA, because the SCF iterations may converge faster [29]. (The slow step is minimizing the atomic positions, and with the BFGS method we use [52] a prior estimate of the Hessian can be exploited so reminimizing after changing the functional from PBE to PBE0 and rescaling the cell is fast.) As such, the on-site method is much faster than methods which use a full or screened calculation of the exact exchange term. The additional cost for doing a TPSS or TPSSh calculation only using the change in the exchange–correlation energy is negligibly small. At least with an all-electron code one could argue that the different functionals should always be used, this would be “good theoretical technique” in the same way that good experimental technique is to check that the results are reproducible and to estimate the errors.

The method we have used to estimate the accuracy, i.e. use the errors for small calibration molecules with different functionals to estimate an error based upon the difference between two (or more in principle) is not perfect, but reasonable; it has been used in a slightly different form earlier with LDA and PW91 functionals [53]. In principle one might be able to do better with a Bayesian method as suggested by Mortensen et al. [54]. The accuracy that we argue the calculations have, ~ 0.25 eV per 1×1 unit cell, is probably the best that can be achieved with current DFT methods. As such these are still some distance from the levels where phonon entropy effects will be important at low temperatures, although they might start to be important at the higher temperatures used in experiments – the kinetics of equilibration for many oxides are slow except at quite elevated temperatures.

The majority of the structures are relatively simple, and most of the energies are not too far from what one might expect based upon basic inorganic chemistry. In general the larger the number of “bonds” between cation and anions, the lower the energy. The

very low energy octahedral Ti structure clearly shows that beyond issues of valence neutrality one needs to consider “conventional” inorganic chemical concepts such as polyhedral packing, as previously suggested for SrTiO₃ (0 0 1) surfaces [13]. While it would be nice to believe that we understand enough about polar oxide surfaces that there are no more surprises to be come, this strongly suggests that we do not.

The two reduced structures which have either an octahedral Ti₂O₃ coverage or a TiO coverage follow rather naturally as co-ordinations where the oxygen sublattice is preserved, and the only difference is which sites are filled by the cations, a common occurrence. It is worth commenting that both of these will show a modulation equal to the [1 1 0] spacing of SrTiO₃, 5.52 Angstroms, if imaged by STM. A slightly larger spacing of 5.9 Angstroms has been reported in a small region [9]. This was interpreted as an octapolar reconstruction of a TiO overlayer and while this is reasonable, it might also have been due to one of these overlayers; more work would be required to determine this. For certain the formation of a TiO phase under highly reducing conditions is consistent with our structures.

The thermodynamics of the SrTiO₃(1 1 1) surface are more complicated than what we have considered; experimentally a range of $n \times n$ reconstructions are found, exactly which forms depending upon the details of the sample preparation. The available Auger data indicates that these are all rich in both Ti and O relative to the fracture surface. In addition, they all show a dominantly strong diffraction spots at, in terms of the 1×1 lattice, a location of approximately (5/3,0) which none of the structures described herein come close to reproducing. The structure of these other reconstructions using both experiments and calculations as well as a more complete thermodynamics is a topic of further publications.

Acknowledgements

LDM acknowledges support from the DOE on Grant No. DE-FG02-01ER45945/A007 and ANC acknowledges support from the DOE on Grant No. DE-FG02-03ER15457. PB and FT acknowledge support from the Austrian Science Foundation, project P20271-N17.

References

- [1] C. Noguera, Journal of Physics: Condensed Matter 12 (2000) R367.
- [2] J. Goniakowski, F. Finocchi, C. Noguera, Reports on Progress in Physics 71 (2008) 016501.
- [3] H. Raebiger, S. Lany, A. Zunger, Nature 453 (2008) 763.
- [4] Y. Haruyama, Y. Aiura, H. Bando, Y. Nishihara, H. Kato, Journal of Electron Spectroscopy and Related Phenomena 88 (1998) 695.
- [5] S. Sekiguchi, M. Fujimoto, M. Nomura, S. Cho, J. Tanaka, T. Nishihara, M. Khang, P. Hyong-Ho, Solid State Ionics 108 (1998) 73.
- [6] A. Gomann, K. Gomann, M. Frerichs, K. Kemper, G.V. Borhardt, W. Maus-Friedrichs, Applied Surface Science 7 (2005) 2053.
- [7] A.N. Chiamonti, Structure and Thermodynamics of Model Catalytic Oxide Surfaces, Evanston, Northwestern, 2005.
- [8] A.N. Chiamonti, C.H. Lanier, L.D. Marks, P.C. Stair, Surface Science 602 (2008) 3018.
- [9] B.C. Russell, M.R. Castell, Journal of Physical Chemistry C 112 (2008) 6538.
- [10] B.C. Russell, M.R. Castell, Physical Review B 75 (2007) 155433.
- [11] A. Pojani, F. Finocchi, C. Noguera, Surface Science 442 (1999) 179.
- [12] A. Pojani, F. Finocchi, C. Noguera, Applied Surface Science 142 (1999) 177.
- [13] N. Erdman, K.R. Poeppelmeier, M. Asta, O. Warschkow, D.E. Ellis, L.D. Marks, Nature 419 (2002) 55.
- [14] P. Blaha, K. Schwarz, G.K.H. Madsen, D. Kvasnicka, J. Luitz, WIEN2k, an Augmented Plane Wave + Local Orbitals Program for Calculating Crystal Properties, Universität Wien, Austria, 2001.
- [15] J.P. Perdew, K. Burke, M. Ernzerhof, Physical Review Letters 77 (1996).
- [16] P. Novák, J. Kuneš, L. Chaput, W.E. Pickett, Physica Status Solidi B – Basic Solid State Physics 243 (2006) 563.
- [17] F. Tran, P. Blaha, K. Schwarz, P. Novák, Physical Review B 74 (2006) 155108.
- [18] J.P. Perdew, M. Ernzerhof, K. Burke, Journal of Chemical Physics 105 (1996).
- [19] C. Adamo, V. Barone, Journal of Chemical Physics 110 (1999) 6158.
- [20] J.M. Tao, J.P. Perdew, V.N. Staroverov, G.E. Scuseria, Physical Review Letters 91 (2003) 146401.
- [21] V.N. Staroverov, G.E. Scuseria, J.M. Tao, J.P. Perdew, Journal of Chemical Physics 119 (2003) 12129.
- [22] J.P. Perdew, Y. Wang, Physical Review B 45 (1992) 13244.
- [23] A.E. Mattsson, D.R. Jennison, Surface Science 520 (2002) L611.
- [24] R. Armiento, A.E. Mattsson, Physical Review B 72 (2005) 085108.
- [25] J.P. Perdew, A. Ruzsinszky, G.I. Csonka, O.A. Vydrov, G.E. Scuseria, L.A. Constantin, X.L. Zhou, K. Burke, Physical Review Letters 100 (2008) 136406.
- [26] V.I. Anisimov, J. Zaen, O.K. Andersen, Physical Review B 44 (1991) 943.
- [27] V.I. Anisimov, F. Aryasetiawan, A.I. Lichtenstein, Journal of Physics: Condensed Matter 9 (1997) 767.
- [28] F. Tran, J. Kuneš, P. Novák, P. Blaha, L.D. Marks, K. Schwarz, Computer Physics Communications 179 (2008) 784.
- [29] L.D. Marks, D.R. Luke, Physical Review B (Condensed Matter and Materials Physics) 78 (2008) 075114.
- [30] F. Silly, D.T. Newell, M.R. Castell, Surface Science 600 (2006) L219.
- [31] J.P. Perdew, A. Ruzsinszky, J. Tao, G.I. Csonka, G.E. Scuseria, Physical Review A 76 (2007) 042506.
- [32] K.S. Jeong, C. Chang, E. Sedlmayr, D. Sulzle, Journal of Physics B – Atomic Molecular and Optical Physics 33 (2000) 3417.
- [33] Z.W. Qu, G.J. Kroes, Journal of Physical Chemistry B 110 (2006) 8998.
- [34] F. Furche, J.P. Perdew, Journal of Chemical Physics 124 (2006) 044103.
- [35] A. Frye, R.H. French, D.A. Bonnell, Zeitschrift Fur Metallkunde 94 (2003) 226.
- [36] J. Carper, Library Journal 124 (1999) 192.
- [37] A.D. Becke, Journal of Chemical Physics 98 (1993) 5648.
- [38] Y. Zhao, D.G. Truhlar, Journal of Chemical Physics 124 (2006) 224105.
- [39] E.R. Johnson, R.M. Dickson, A.D. Becke, Journal of Chemical Physics 126 (2007) 184104.
- [40] A. Ramirez-Solis, Journal of Chemical Physics 126 (2007) 224105.
- [41] K.E. Riley, K.M. Merz, Journal of Physical Chemistry A 111 (2007) 6044.
- [42] R.F.W. Bader, Atoms in Molecules – A Quantum Theory, Oxford University Press, Oxford, 1990.
- [43] C. Adamo, M. Ernzerhof, G.E. Scuseria, The Journal of Chemical Physics 112 (2000) 1643.
- [44] A.D. Rabuck, G.E. Scuseria, Theoretical Chemistry Accounts: Theory Computation and Modeling (Theoretica Chimica Acta) 104 (2000) 439.
- [45] B. Jiang, J.M. Zuo, N. Jiang, M. O’Keeffe, J.C.H. Spence, Acta Crystallographica Section A 59 (2003) 341.
- [46] Available from: <http://www.wien2k.at/Depositary/SurfSci_STO111_Marks/>.
- [47] I. Batyrev, A. Alavi, M.W. Finnis, Ab initio calculations on the Al₂O₃2(0 0 0 1) surface, Meeting on the Surface Science of Metal Oxides, 1999, p. 33.
- [48] K. Reuter, M. Scheffler, Physical Review B 65 (2002) 035406.
- [49] K. Johnston, M.R. Castell, A.T. Paxton, M.W. Finnis, Physical Review B 70 (2004) 085415.
- [50] E. Heifets, S. Piskunov, E.A. Kotomin, Y.F. Zhukovskii, D.E. Ellis, Physical Review B 75 (2007) 115417.
- [51] O. Warschkow, Y.M. Wang, A. Subramanian, M. Asta, L.D. Marks, Physical Review Letters 100 (2008) 86102.
- [52] J. Rondinelli, D. Bin, L.D. Marks, Computational Materials Science 40 (2007) 345.
- [53] C.H. Lanier, J.M. Rondinelli, B. Deng, R. Kilaas, K.R. Poeppelmeier, L.D. Marks, Physical Review Letters 98 (2007) 086102.
- [54] J.J. Mortensen, K. Kaasbjerg, S.L. Frederiksen, J.K. Nørskov, J.P. Sethna, K.W. Jacobsen, Physical Review Letters 95 (2005) 216401.